Supplementary Material (ESI) for Journal of Materials Chemistry

Stable anchoring of dispersed gold nanoparticles on hierarchic porous silica-based materials

Mónica Pérez-Cabero, Jamal El Haskouri, Benjamín Solsona,* Isabel Vázquez, Ana Dejoz, Tomás García, Jesús Álvarez-Rodríguez, Aurelio Beltrán, Daniel Beltrán and Pedro Amorós*

SUPPLEMENTARY INFORMATION

Synthesis and characterization of the CoOx-UVM-7 supports

All the synthesis reagents (tetraethyl ortosilicate (TEOS), $CoCl_2$, triethanolamine ($N(CH_2-CH_2-OH)_3$, hereinafter TEAH3) and hexadecyltrimethylammonium bromide (CTMABr) are analytically pure, and were used as received from Aldrich. CoO_x-UVM-7 supports were prepared by a modified atrane route.[1] The general aspects of this one-pot surfactant assisted procedure for synthesizing nanoparticulate bimodal mesoporous silicas were previously described.[2] In a typical synthesis to obtain the support with Si/Co= 50, a mixture of TEOS (11.5 mL; 0.05 mol), $CoCl_2$ (0.24 g; 0.001 mol) and TEAH3 (23 mL, 0.17 mol) was heated at 150ºC for 10 min to prepare atrane complexes in TEAH3 medium. The resulting solution was cooled down to 90 °C, and 4.68 g CTMABr (0.01 mol) were added. Then, 80 mL of water were slowly added with vigorous stirring at 80 °C. After a few minutes, a white suspension resulted that was aged at room temperature for 4 h. The resulting mesostructured solid was then separated by centrifugation, washed with water and ethanol, and air dried. To obtain the final catalyst, the as-synthesized solid was calcined at 500 °C for 4 h under a static air atmosphere.

The results of the magnetic measurements and UV-Vis spectra recorded on hydrated and dehydrated samples confirm that the Co species are present in the form of CoO_x nanodomains, as occurs in the case of the MO_x-MCM-41 and MO_x-UVM-7 materials previously described.[3] Magnetic measurements show that the particle size remains constant, independently of the Si/Co molar ratio. Thus, both samples show an identical superparamagnetic behaviour: (i) a sharp increase

of the DC magnetic susceptibility below *ca*. 12-17 K, (ii) a frequency dependent AC signal with maxima at 4-7 K in the in-phase signal (χ') and at 3-5 K in the out of phase signal (χ") (Figure S1), (iii) deviations in the zero field cooled and field cooled susceptibilities below ca. 10-15 K, with a remnant magnetization that vanishes at *ca*. 15 K for all the samples, and (iv) hysteresis cycles in the isothermal magnetization at low temperatures.

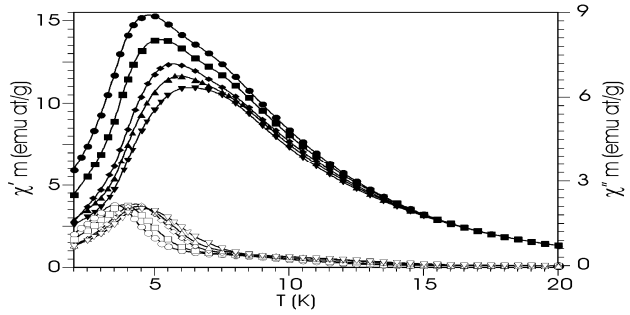

Figure S1.- Thermal variation of the in-phase (filled symbols; left scale) and the out-of-phase signals (empty symbols; right scale) of the AC susceptibility of sample 1 at (!) 1 Hz, (#) 10 Hz, (♦) 110 Hz, (▲) 330 Hz and (▼) 995 Hz.

A way to estimate the particle size uses the activation energy (E_a= 105 and 104 K for samples 1 and 2, respectively) obtained from the Arrhenius fit of the frequency-dependent maxima in χ" (T_m), as the activation energy E_a = K.V, where K is the energy density of the magnetic anisotropy (K = $3.8.10^6$ erg.cm^{-3})[4] and V the particle volume.[5] From this approach we can estimate particle sizes of *ca.* 2.9 nm for both samples.

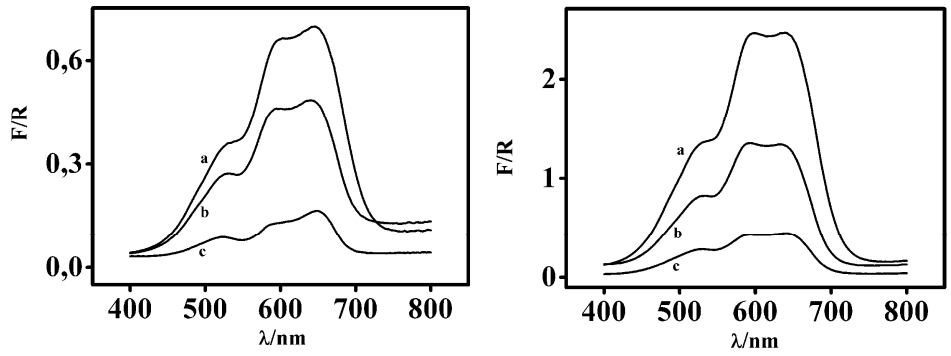

Figure S2.- Diffuse reflectance UV-visible spectra of the samples 1 (left) and 2 (right). (a) Dehydrated samples. (b) As-prepared materials. (c) Hydrated samples.

Shown in Figure S2 are the UV-Vis spectra of CoO_x-MCM-41 samples dehydrated at 400ºC under air atmosphere. The spectra display a significant absorption in the VIS region with three maxima at *ca.* 15000, 17000 and 19000 cm^{-1} that can be unambiguously assigned to the $^4A_2(F) \rightarrow {}^4T_1(P)$ transition of cobalt(II) ions in tetrahedral oxygen sites.[6] The intensity of this band significantly decreases by hydration, and it recovers reversibly by posterior drying. Taking into account the large difference between the absorption molar coefficients of the bands associated to octahedral *vs.* tetrahedral Co(II) sites, it can be reasonably assumed that the area under the VIS curve is proportional to the number of no-hydrated tetrahedral cobalt centres. Under this simplification, we can estimate a ratio of water accessible to inaccessible Co ions close to 9/2 practically constant irrespective of the cobalt content. This behaviour clearly indicates that a proportion of tetrahedral cobalt atoms remain unaltered in the core of the particles or at the silica-CoO_x inter-phase which indicate that the CoO_x domains are partially embedded in the silica walls.

Mesoporosity of the CoO_x-UVM-7 supports is illustrated by the N_2 adsorption-desorption isotherms (Figure S3). As can be noted, the curves show two adsorption steps. The first step, which appears well-defined in all cases at intermediate partial pressures ($0.2 < P/P_0 < 0.5$) is characteristic of Type IV isotherms and can be related to capillary condensation of N_2 inside the uniform mesopores. The sharp curvature of the isotherms is consistent with narrow pore size distributions. The second adsorption at relatively high P/P_0 values > 0.8 is associated to the filling of the inter-particle voids. In Table S1 are gathered the values of BET surface area, pore size and volume (by application of the BJH model) and an estimation of the mesopore wall thickness. The thickness of the pore walls (Wt = a_0-ØBJH) increases with the Co content, which is consistent with the incorporation of CoO_x particles to the silica mesostructure.

Taking into account several factors such as (1) the relative size of the CoO_x nanoparticles, the mesopore diameter and pore wall thickness, and (2) the relatively small decrease in BET area

and pore volume of the cobalt containing silicas when compared to the pure parent UVM-7 material, all samples really can be considered as high surface area materials without significant pore blocking associated to the incorporation of CoO_x nanoparticles.

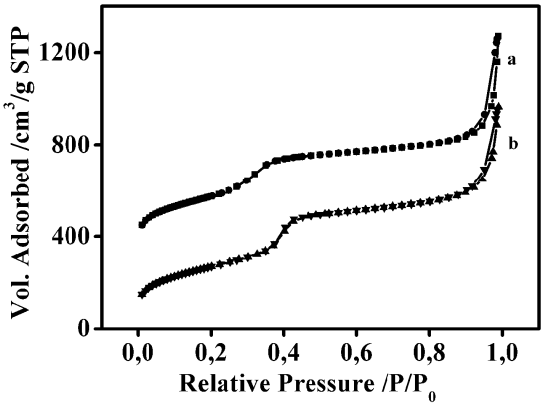

Figure S3.- N_2 adsorption-desorption isotherms for: (a) sample 2, (b) sample 1.

Table S1- Selected Physical data for CoO_x-UVM-7 supports and the parent UVM-7 pure silica.

Sample	a_0 /nm	Small pore size /nm	Large pore size /nm	Total pore volume /cm^3g^{-1}	Pore Wall /nm
UVM-7	5.05	3.05	43.2	2.49	2.00
1	5.35	2.98	42.5	1.65	2.37
2	5.55	2.71	33.4	1.53	2.84

Stability of the CoO_x-UVM-7 support

We have recorded the XRD pattern (Figure S4) and the N_2 adsorption-desorption isotherm (Figure S5) of a CoO_x-UVM-7 (Sample 2) after treating this sample in a water solution at pH= 10 during 1 hour at room temperature. This study has been carried out in order to evaluate the support degradation during the gold incorporation step. As can be observed, only a small decrease in the (100) XRD peak of *ca.* 15% occurs after treating. This fact and the observed resolution decrease indicate that a certain order loss occurs after NaOH-treatment, as expected. In any case, the Figure

S5 displays that the bimodal mesoporous character of the UVM-7-like support is preserved with only slight loss of BET area and pore volume (S_{BET}= 815.8 m^2/g; BJH Pore Vol. = 1.31 cc/g).

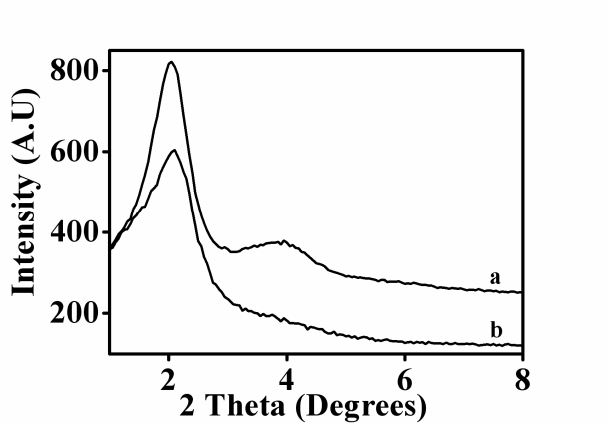

Figure S4.- XRD pattern of Sample 2 as prepared (a) and after treatment at pH= 10 during 1 hour.

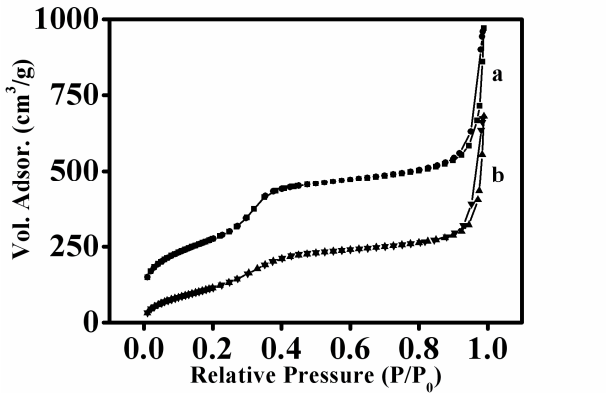

Figure S5.- N_2 adsorption-desorption isotherms of Sample 2 (a) before and (a) after treatment at pH= 10 during 1 hour.

References

1 S. Cabrera, J. El Haskouri, C. Guillem, J. Latorre, A. Beltrán, D. Beltrán, M. D. Marcos and P. Amorós, *Solid State Sci.,* 2000, **2**, 405.

2 J. El Haskouri, J. M. Morales, D. Ortiz de Zárate, L. Fernandez, J. Latorre, C. Guillem, A. Beltrán, D. Beltrán and P. Amorós, *Inorg. Chem.,* 2008, **47**, 8267.

3 (a) J. El Haskouri, S. Cabrera, C. J. Gómez-García, C. Guillem, J. Latorre, A. Beltrán, D. Beltrán, M. D. Marcos and P. Amorós, *Chem. Mater.*, 2004, **16**, 2805; (b) J. El Haskouri, S. Cabrera, M. Caldés, J. Alamo, A. Beltrán, M. D. Marcos, M.D., P. Amorós and D. Beltrán, *Int. J. Inorg. Mater.*, 2001, **3**, 1157; (c) L. Fernández, N. Carró, J. El Haskouri, M. Pérez-Cabero, J. Alvarez-Rodríguez, J. Latorre, C. Guillem, A. Beltrán, D. Beltrán and P. Amorós, *Nanotechnology*, 2008, **19**, 225603; (d) J. El Haskouri, L. Dallali, L. Fernández, N. Garró, S. Jaziri, J. Latorre, C. Guillem, A. Beltrán and P. Amorós, *Physica E*, 2009, **42**, 25.

4 (a) A. E. Hughes, *Phys. Rev.*, 1971, **3**, 877. (b) M. Gruyters, *J. Magn. Magn. Mater.*, 2002, **248**, 248.

5 S. Takada, M. Fujii, S. Kohiki, T. Babasaki, H. Deguchi, M. Mitome and M. Oku, *Nano Letters* 2001, **1**, 379.

6 A. A. Verberckmoes, B. M. Weckhuysen and R. A. Schoonheydt, *Microp. Mesop. Mater.* 1998, **22**, 165 and references therein